Research

Ecography 39: 954–960, 2016
doi: 10.1111/ecog.02055

Subject Editor: Ken Kozak. Editor-in-Chief: Jens-Christian Svenning. Accepted 3 November 2015

Historical dynamics of *Batrachochytrium dendrobatidis* in Amazonia

C. Guilherme Becker, David Rodriguez, Carolina Lambertini, L. Felipe Toledo and Célio F. B. Haddad

C. G. Becker (cgb58@cornell.edu) and C. F. B. Haddad, Departamento de Zoologia, Univ. Estadual Paulista, Rio Claro, SP 13506-900, Brazil. – D. Rodriguez, Dept of Biology, Texas State Univ., San Marcos, TX 78666, USA. – C. Lambertini and L. F. Toledo, Depto de Biologia Animal, Univ. Estadual de Campinas, Campinas, SP 13083, Brazil.

The Amazon forest is known for its astonishing amphibian diversity, yet the potential distribution and underlying impacts of the most important amphibian pathogen is unknown for most of Amazonia. In this retrospective survey of preserved *Leptodactylus* frogs, collected over a 119 yr period, we used quantitative PCR to detect the fungal pathogen *Batrachochytrium dendrobatidis* (*Bd*) and performed spatial scan analyses to identify spatiotemporal clusters of *Bd*. We also quantified the potential effect of environmental factors on the likelihood of *Bd* occurrence and generated an updated suitability map for *Bd* in the Amazon that included our retrospective sampling. We detected *Bd* in lowland Amazon as early as 1935, in the state of Pará, Brazil, and we found low prevalence (~ 3.8%) over time. We identified two statistically significant spatiotemporal clusters of *Bd*: a recent and narrow cluster in the Amazon River delta and a spatiotemporally broad cluster in the southern edge of Amazon and Brazilian savanna. Furthermore, we found an increase in *Bd*-positive samples in the southwestern Amazon after the 1990s, coinciding with reported amphibian declines in neighboring high elevation sites on Andean slopes of Peru. Spatial regressions indicated that higher human interference, higher precipitation, and lower temperatures were significant predictors of *Bd* occurrence. Environmental niche modeling predicted some narrow areas of suitable climates along the Amazon's periphery and generally low climatic suitability for *Bd* in the central Amazon; although, we found clusters of *Bd*-positive samples with unexpectedly high infection loads in areas of predicted low suitability. Our study indicates that accelerated human development may put Amazonian amphibians at risk from *Bd* introductions, and it highlights the potential need to monitor *Bd* dynamics near Amazonian port cities.

The Amazon is the world's largest tropical rainforest and harbors over a thousand amphibian species (IUCN et al. 2015). Accelerated deforestation in lowland Amazonia poses a threat to the local anurofauna, but reports of population declines are still scarce for lowland amphibian species (McCracken et al. 2009, Deichmann et al. 2010). The lack of reports can be attributed to large parts of the Amazon still being remote and inaccessible for research, or because much of its original extent still remains intact (IBGE 2015). However, several high-elevation sites along the Andean slopes bordering the Amazon show recent patterns of drastic amphibian population declines with many of them linked to the emergence of the frog-killing fungus *Batrachochytrium dendrobatidis* (*Bd*) (Lampo et al. 2006, Lips et al. 2008, Catenazzi et al. 2011, Menendez-Guerrero and Graham 2013).

Amphibian declines attributed to *Bd* have been reported on several continents (Fisher et al. 2009). Examples of the most dramatic declines and extinctions include an epizootic wave of chytridiomycosis moving through pristine high-elevation forests of Central America, causing local population declines of several amphibian species (Berger et al. 1998, Lips et al. 2008, Cheng et al. 2011). It is also likely that multiple introductions of a hypervirulent *Bd* strain into South America are linked to recent population declines at pristine and topographically complex sites that border the western Amazon basin (Lampo et al. 2006, Lips et al. 2008, Catenazzi et al. 2011, Menendez-Guerrero and Graham 2013). For example, in Manu National Park (Peru) local extinctions at montane forest sites above an elevation of 1200 m were attributed to the emergence of *Bd* in the early 2000s (Catenazzi et al. 2011).

Lowland species, however, have not shown demographic patterns of recent declines (Deichmann et al. 2010), yet *Bd* was recently detected at lowland sites at the borders of the Amazon (McCracken et al. 2009, Courtois et al. 2015, Valencia-Aguilar et al. 2015), suggesting that this pathogen could be also present in the central Amazon. Niche models predict low suitability for *Bd* in most of lowland Amazon Basin (Ron 2005, Rödder et al. 2009, Liu et al. 2013), but lowland resistant species may potentially spread the pathogen at faster rates than their susceptible highland counterparts

(Rodriguez-Brenes et al. pers. comm.). Therefore, highland areas in the northern Amazon (e.g. state of Roraima in Brazil and Bolivar state in Venezuela) could also be at higher risk for outbreaks propagated though lowland species.

Besides the high habitat connectivity that may facilitate pathogen dispersal between the Andean and central Amazon, *Bd* could also be arriving through the southern or eastern borders. A recent study shows that the Brazilian Atlantic forest has long-term endemicity of at least two *Bd* strains (Rodriguez et al. 2014). Thus, *Bd* could extend from the Atlantic forest through the Brazilian Savanna (Cerrado) to the Amazon. Savanna environments, however, may act as a pathogen dispersal barrier because *Bd* is significantly suppressed in dryer areas of open-canopy (Becker and Zamudio 2011, Puschendorf et al. 2011). Therefore, comprehensive retrospective spatial surveys are needed to understand the historical dynamics of *Bd* in Amazonia, where disease outbreaks or silent declines could be happening in remote areas.

Several studies have used retrospective surveys to describe *Bd* pathogen dynamics in many regions (Weldon et al. 2004, Ouellet et al. 2005, Soto-Azat et al. 2010, Cheng et al. 2011, Vredenburg et al. 2013, Rodriguez et al. 2014, Courtois et al. 2015, Talley et al. 2015). Here, we used quantitative PCR to detect *Bd* on preserved anurans collected over a 119 yr period. Using these presence/undetected data, we then performed spatial scan analyses to detect spatiotemporal clusters of *Bd*. To test whether *Bd* is spatiotemporaly present, absent or spreading, we focused our survey on *Leptodactylus*, a Neotropical genus of frogs with several highly aquatic species (de Sá et al. 2014). We then quantified the potential role of climate (i.e. temperature and precipitation), human footprint, and vegetation density on the likelihood of *Bd* occurrence. Given the current lack of spatial information for *Bd* in Amazon, we also used a maximum entropy method to provide an updated suitability map for *Bd* across the entire biome.

Methods

Sampling and qPCR

We sampled 1391 post-metamorphic preserved anuran specimens from Amazonia and adjacent ecoregions collected from 1895 to 2014. We focused our sampling on species of *Leptodactylus* (43 species; Supplementary material Appendix 1, Table A1) owing to their generally highly aquatic habits (de Sá et al. 2014), endemicity to the Neotropics, wide abundance across the biome, and known records of *Bd* infections in the wild (Rodriguez et al. 2014). These specimens were housed in collections at the American Museum of Natural History (AMNH) and the Brazilian collections: Museu de Zoologia 'prof. Adão José Cardoso', Univ. Estadual de Campinas (ZUEC), Museu de Zoologia, Univ. de São Paulo (MZUSP), Museu Nacional, Rio de Janeiro (MNRJ), Coleção Herpetológica 'Eugenio Izecksohn', Univ. Federal Rural do Rio de Janeiro (UFRRJ), Coleção de Anuros Sérgio Potsch – Univ. Federal do Rio de Janeiro (UFRJ), Coleção de Anuros Célio F. B. Haddad – Univ. Estadual Paulista (CFBH), Museu Paraense Emilio Goeldi (MPEG), and Museu de Zoologia, Univ. Federal do Acre (UFAC) (Supplementary material Appendix 1, Table A1). We inferred approximate GPS coordinates in decimal degrees for all specimens based on the recorded collection locality. For specimens that did not have specific location data, we used the collection municipality centroid as the coordinates. To swab for *Bd*, we followed the same procedures as in Rodriguez et al. (2014); wherein we rinsed each individual with new 70% ethanol, allowed the specimen to briefly dry on a clean tray, and then swabbed them using standardized methods and Medical Wire swabs (MW113) (Hyatt et al. 2007, Cheng et al. 2011). We placed the skin swabs in sterile L233052 1.5 ml screw-top centrifuge tubes with o-rings (Laboratory Products Sales) and then allowed the swabs to dry completely before attaching the cap.

Using 50 µl of Prep-Man Ultra per swab (Hyatt et al. 2007), we extracted DNA by first agitating the tube plus solution for 1 min, boiling for 10 min, and then cooling for 2 min. We then centrifuged the tube at 13 000 rpm for 1 min, after which we inverted the swab with flame-sterilized tweezers before centrifuging the tube at 13 000 rpm for 5 min and then discarding the swab. We centrifuged the tube at 13 000 rpm for 10 min before taking 4 µl of extract from just below the meniscus and placing it into 36 µl of nuclease-free water. We used this dilution as the template for the qPCR reactions.

For *Bd* detection (positive or undetected), we used a StepOnePlus real-time PCR system (Applied Biosystems) following the procedures described in Rodriguez et al. (2014). For cost efficiency, we performed qPCRs in singlicate to facilitate increased sampling size. Our standard curve had a dynamic range of 0.1 to 1000 genomic equivalents (GE) and was made from extracts of strain CLFT023 isolated from Brazil (Vieira et al. 2012). We categorized each sample as *Bd* positive when zoospore genome equivalents were ≥ 1 (Kriger et al. 2007).

Analysis of prevalence

We calculated prevalence as the proportion of *Bd*-positives samples in a particular temporal or spatial category. We grouped each sampled specimen into temporal intervals of 25 yr and compared average prevalence over time using 95% binomial confidence intervals (CI) with a logistic (logit) parameterization obtained using the binom function from the binom.confint package in R (R Development Core Team).

Spatiotemporal scan analysis

Using SatScan ver. 9.1.1 (Kulldorff 2009), we preformed purely spatial and space-time scan analyses, similar to the methods in Rodriguez et al. (2014), by applying Kulldorff's clustering algorithm (Kulldorff 1997) under a Bernoulli probability model. For the space-time analysis, we set the maximum temporal cluster size at 50% of the population and time aggregation at 25 yr. This method places a variable circular window on each collection locality, with the algorithm evaluating positive and negative counts in each space-time cluster. The clusters are compared to the entire

landscape using maximum-likelihood ratio statistic to infer statistical significance for the most likely clusters. We then used general linear models (GLMs; standard least square) to compare average infection loads among significant clusters.

Effects of abiotic factors on *Bd* spatial distribution

We performed autologistic regressions (AUTOLOG), while accounting for spatial autocorrelation, to measure the potential effects of climate (i.e. temperature and precipitation), human footprint, and vegetation density on *Bd* occurrence (positive vs undetected) in Amazonian *Leptodactylus*. We extracted data on 11 temperature variables (bio1–bio11) and 8 precipitation variables (bio12–bio19; Hijmans et al. 2005), human footprint (Sanderson et al. 2002), and vegetation density (USGS and FAO 2000) for each sampling location at 1 km resolution using Arc Map ver. 10.1 (ESRI 2012). We used principal component analysis to consolidate bioclim variables owing to their high cross-correlation, and we used the scores of the first principal component axis (PC) depicting temperature and precipitation as variables in downstream model selection procedure. We used AUTOLOG multi-model inference, including sets of the aforementioned explanatory variables and *Bd* (presence/undetected) as the response variable (Rangel et al. 2010). We tested ~ 300 meaningful models including one-level interactions. We ranked competing models based on Akaike information criterion (AIC) and reported the most parsimonious model.

Ecological niche modeling

We used the same 19 bioclimatic predictor variables described above to develop spatial distribution models for *Bd* in Amazonia using the maximum entropy method MaxEnt (3.3.3e; <www.cs.princeton.edu/~schapire/maxent/>, accessed 20 October 2011; Elith et al. 2006). We compiled a database of published records of *Bd* occurrence locations for South America (Supplementary material Appendix 1). Because *Bd* strains can vary in environmental tolerance (Stevenson et al. 2013), we did not include *Bd* occurrence locations from other continents in our analyses. Furthermore, we did not include variables such as vegetation density and human footprint in our niche modeling, because *Bd* sampling is biased to areas of higher human influence, thus climate alone is preferable in these situations (Beaumont et al. 2005). MaxEnt models minimize relative entropy between the probability of presence data and that of the background landscape. This method is often preferred over traditional presence–absence methods, and therefore widely used among evolutionary ecologists (Elith et al. 2011).

We employed a MaxEnt method that randomly sets aside 25% of our sampling locations to estimate model accuracy. Because the model including all bioclimatic variables (full model) is usually redundant and over-fitted (Elith et al. 2011), we generated a model including only the most important variables (pruned model). To achieve this goal, we removed variables that contributed less than 3% to the full model and checked for cross-correlation among the remaining variables. Our bioclimatic variables were ranked based on their AUC (the area under curve of the receiver operating characteristic). The AUC is a sensitive metric of model predictive power and measures the performance of the model to correctly classify a species as present or absent in random locations. AUC values range between 0.5 (not better than random) and 1 (perfect prediction), and models with values over 0.8 are considered high-accuracy models (Araujo and Guisan 2006). We used the full set of presence records to plot *Bd* probability distribution map for the Amazon region using the pruned MaxEnt model including the top ranking variables.

Data available from the Dryad Digital Repository: <http://dx.doi.org/10.5061/dryad.h3112> (Becker et al. 2015).

Results

We detected *Bd* in lowland Amazon as early as 1935 in the state of Pará, Brazil, though our earliest positive record was from 1895 at the northern edge of the Venezuelan Amazon. We found temporally constant and low *Bd* prevalence (average of 3.81%) with no significant peaks across time when considering the entire dataset (Fig. 1). Even though we did not detect clear patterns of spread through time, we did detect two significant spatial clusters of *Bd*-positive samples in the east and south, in addition to a broad *Bd*-undetected area encompassing the remote central Amazon (Fig. 1). We also detected more *Bd*-positive samples in southwest Amazon regions after the 1990s (Fig. 2; Supplementary material Appendix 1, Table A1). The most significant spatial aggregation of *Bd* occurred at a single location in the Amazon River delta, state of Amapá, Brazil [(cluster A: all 7 samples from 2008 testing positive for *Bd* (log-likelihood ratio = 23.301; $p < 0.001$) and showing high zoospore loads (average GE = 2206.88)]. The second significant cluster (cluster B) is much broader spatiotemporally (587.82 km radius; 17 positives samples ranging from 1962 to 2010; log-likelihood ratio = 12.921; $p < 0.001$), with significantly lower infection loads (average GE = 123.64) than *Bd* positives from cluster A ($t = 3.28$, $p = 0.003$), and is located in the southern edge of the Amazon and Brazilian Savanna. We performed SatScan analyses for 25-yr temporal aggregations and the same two significant clusters varied slightly in area (Supplementary material Appendix 1, Table A2).

Spatial regressions indicated that climate, human footprint, and vegetation density were all important predictors of *Bd* in the Amazon region ($\chi^2 = 91.317$, $n = 1391$, $p < 0.001$; Table 1). Specifically, milder temperatures, higher precipitation, higher vegetation density, and higher human footprint were significant predictors of *Bd* occurrence. Environmental niche modeling also confirmed that central Amazon has climatic conditions with low suitability for *Bd*, even though we detected narrow areas with suitable climates throughout Amazon's periphery (Fig. 3). The reported pruned MaxEnt model included the following seven bioclimatic variables representing 91.2 % of the explanatory power in the full model: isothermality (Bio3; 20.6%), temperature seasonality (Bio4; 6.4%), maximum temperature of the warmest month (Bio5; 35.9%), mean temperature of the driest quarter

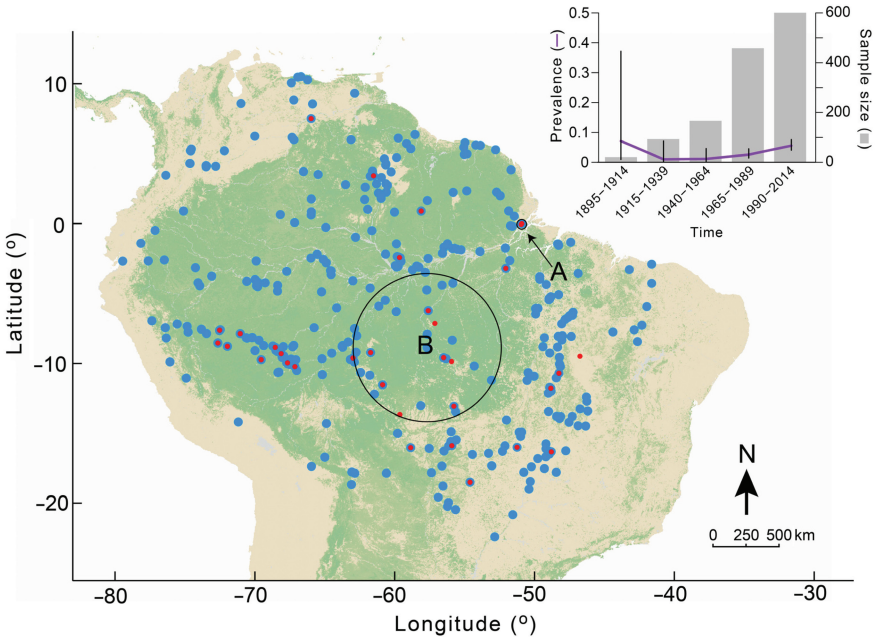

Figure 1. Amazon forest and adjacent ecoregions with the geographical distribution of *Bd*-positive (red) and *Bd*-undetected museum specimens (blue) collected from 1895 to 2014. *Bd* prevalence (purple line) with 95% binomial confidence intervals and sample size (grey bars) are reported for 25-yr intervals. Significant clusters of *Bd* positive samples are shown (A, B). Background depicts vegetation density ranging from low (yellow) to high (green).

(Bio9; 4.7%), precipitation of the wettest quarter (Bio16; 10.1%), precipitation of the warmest quarter (Bio18; 10.5%), and precipitation of the coldest quarter (Bio19; 3.0%). The reported pruned model (AUC = 0.879 ± 0.022 SD) showed similar AUC values when compared to the full model (AUC = 0.894 ± 0.019 SD).

Discussion

Our study demonstrates low prevalence of *Bd* in eastern and peripheral lowland Amazon regions over the last 80 yr, thus closing a large sampling gap in *Bd* spatial ecology for South America. Furthermore, we found a narrow and highly significant cluster including several samples with high infection loads in Macapá, a port city on the Amazon delta, which suggests that recent introductions are potentially occurring and could pose a threat to the local anurofauna. Additionally, we detected an increase in *Bd*-positive sites in the southwestern lowlands after the late 1990s, which suggests that *Bd* strains associated with amphibian declines may be spreading from Peru to central Amazon (Catenazzi et al. 2011). Yet, we failed to detect *Bd* in northwestern lowlands despite

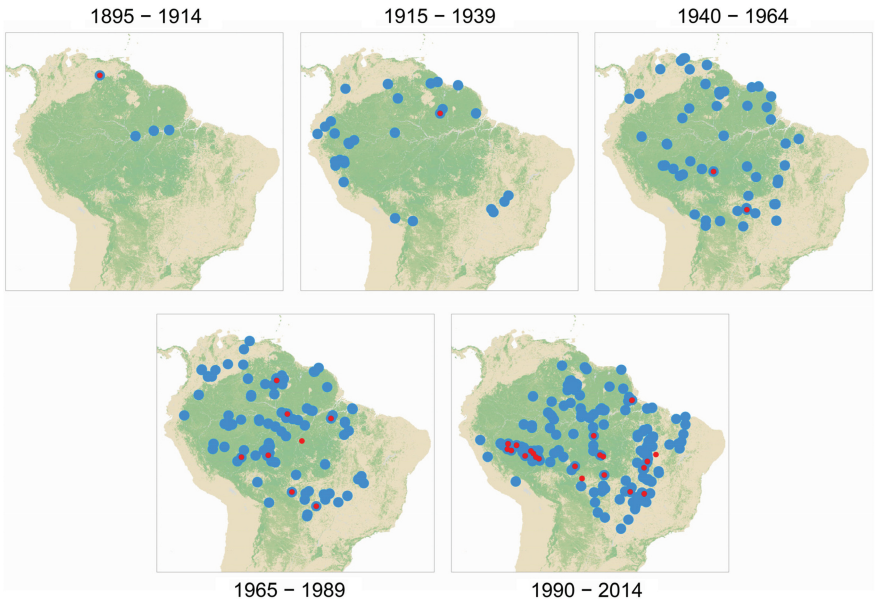

Figure 2. Spatiotemporal distribution of *Bd*-positive (red) and *Bd*-undetected (blue) samples in the Amazon forest and adjacent ecoregions.

Table 1. Autologistic regression testing simultaneously the effects of climate (PC1, PC2), human footprint, and vegetation density on *Bd* occurrence in amphibians from Amazonia and adjacent ecotones.

Variable	Std. coeff.	*t*	p
Constant	0	–7.499	< 0.001
Spatial autocovariate term (*yW*)	2.635	6.45	< 0.001
i) Climate PC1	–5.705	–3.258	0.001
ii) Climate PC2	3.582	2.025	0.043
iii) Human footprint	2.691	1.982	0.048
iv) Vegetation density	2.751	1.686	0.092
i × iii	5.473	3.046	0.002
ii × iii	–2.232	–1.314	0.189
iii × iv	–3.863	–2.378	0.017

*Climate PC1 and climate PC2 consolidating 11 metrics of temperature (Bio1–Bio11) and 8 metrics of precipitation (Bio12–Bio19) accounted for 48.6 and 22.9% of the variation in the original variables, respectively.

extensive sampling, which supports previous predictions that constant high temperatures and relatively low human influence make the remote central Amazon a potential safe haven from amphibian chytridiomycosis (Liu et al. 2013).

Our retrospective survey indicates that Amazonian *Leptodactylus* show *Bd* prevalence one order of magnitude lower than that observed for anurans from Brazil's Atlantic forest during a comparable period of time (Rodriguez et al. 2014). This is not surprising given that the Atlantic forest encompasses a larger area of *Bd* optimum climatic envelope when compared to the Amazon (see high congruence between Fig. 3 and Liu et al. 2013). Nevertheless, we now know that strains vary in their thermal optima (Stevenson et al. 2013), and if *Bd* GPL was introduced into South America during the last few hundred years as suggested by contemporary population genetics of *Bd* strains (James et al. 2015), a century (which could be equivalent to ~ 9000 generations of *Bd*) could have been enough time for the pathogen to adapt to warmer climates and persists endemically (Voyles et al. 2012). Further studies focusing on genotyping Amazonian *Bd* could elucidate its origins and whether or not this pathogen shows strong local adaptation. These studies could help explain the observed long-term low prevalence and endemicity seen in parts of our sampled area.

Even though *Bd* persists with low prevalence in the Amazon, we observed an increase in *Bd*-positive sites during the 1990s on the border of Brazil and Peru, suggesting that an introduced *Bd* strain could be spreading from the Peruvian Andes to lowland Brazilian Amazon. Specifically, we detected positive sites along the Brazilian state of Acre, which is located ~ 160 km east from Manu National Park where amphibian declines were reported around early 2000s (Catenazzi et al. 2011). Furthermore, our spatial scan analysis detected two recent and highly significant clusters of *Bd*-positives denoting higher local prevalence. The narrow cluster we detected in the state of Amapá could be a recent point of introduction. These *Bd*-positive samples also showed infection loads one order of magnitude higher than positives from the other significant cluster, suggesting a localized outbreak. A second scenario is a punctuated increase in host susceptibility due to climate fluctuations or environmental stress (Pounds et al. 2006, Rohr et al. 2008, Rohr and Raffel 2010). Our spatial regression analysis also supports this second less likely possibility, as *Bd* occurrence increased towards areas of higher human interference (i.e. human footprint). Further studies sampling live frogs around this port

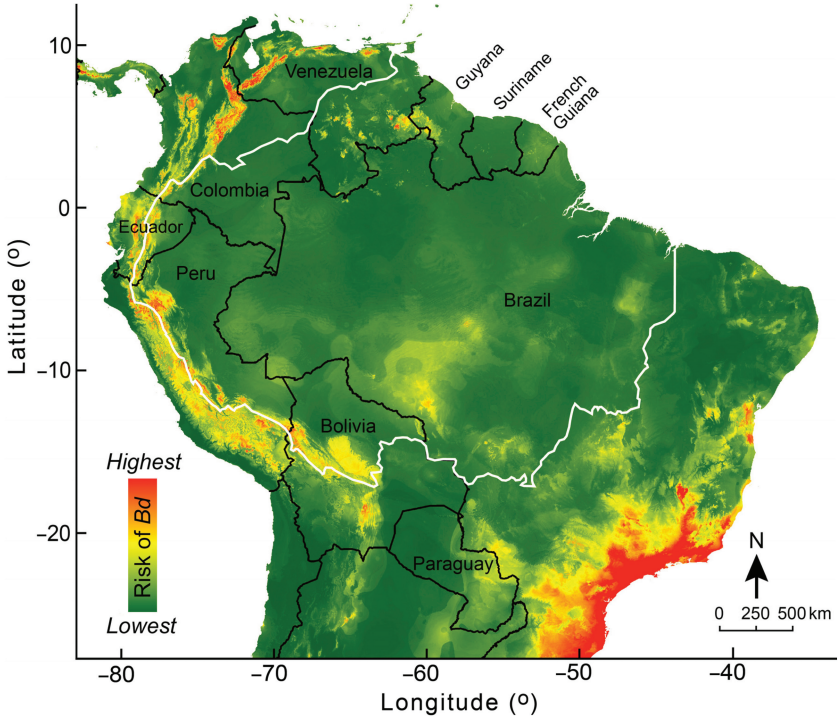

Figure 3. Likelihood of occurrence of *Batrachochytrium dendrobatidis* based on bioclimatic variables of temperature and precipitation. The reported pruned MaxEnt model included 4 temperature and 3 precipitation metrics. Country boundaries in black and international Amazon boundaries in white.

city, and others, are needed to survey for potential sites of introduction and possibly evaluate the consequences of those introductions.

The second cluster we detected is much broader and located at the southeastern edge of the Amazon forest in the Brazilian states of Rondônia and Mato Grosso. Our *Bd* distribution model based on optimum climatic envelope suggests that, together with the Tepuis at north and the Andean slopes, this region exhibits suitable climates for *Bd*. Our results also confirm earlier predictions of global distribution models for *Bd* (Ron 2005, Rödder et al. 2009, Liu et al. 2013, James et al. 2015) in which the remote central Amazon is less suitable for *Bd* persistence or introductions owing to its warmer climates and minimal human interference. However, the high explanatory power of human footprint in our spatial regressions points to potential re-introductions of *Bd* in developing Brazilian cities. At the same time that anthropogenic disturbances to natural vegetation should reduce *Bd* prevalence and disease risk at the local scale, due to a reduction in canopy density and shifts in microclimates (Raffel et al. 2010, Becker and Zamudio 2011, Puschendorf et al. 2011, Becker et al. 2012), human footprint can enhance *Bd* spread through commercial trade and introduction of exotic amphibian hosts (Schloegel et al. 2012, Liu et al. 2013). Our spatial regressions also showed that human footprint, vegetation density, and climate could synergistically interact and exacerbate disease risk. For instance, the narrow *Bd* cluster (A) detected at the edge of the lowland port city of Macapá is unexpected in terms of optimal climates for the pathogen, and might represent interactions between high vegetation densities and high human influence.

In summary, we show that remote central Amazon is likely *Bd*-free, which bodes well for amphibian conservation. Our combined results, however, indicate that accelerated human development may put Amazonian amphibians at risk with *Bd* introductions, especially in areas of microenvironmental suitability for the pathogen such as the Brazilian states of Rondônia, northern Roraima, and northern Mato Grosso. As most of industrialized Brazil is located in the domains of the Atlantic forest (120 million people; 70% of Brazil's population), a variety of goods transported from there to the Amazon region may potentially carry viable *Bd* zoospores (Rodriguez et al. 2014). Because the Atlantic forest harbors two known Global Pandemic Lineages of *Bd*-GPL (i.e. *Bd* GPL-1 and *Bd* GPL-2; James et al. 2015), large cities in the Amazon are more at risk of introductions of hypervirulent *Bd*-GPL strains. To further assess these potential risks, experimental infection studies testing the pathogenicity of Atlantic forest *Bd* strains on Amazonian amphibian species under their native warm and humid microclimates would be useful. Finally, our study highlights the need to monitor amphibian disease risk in areas of suitable climates for *Bd* near major port cities such as Manaus, Belém, and Macapá. Our findings provide target areas for further study of *Bd* pathogen dynamics, which can in turn assist amphibian conservation and management efforts of wild amphibian populations in one of the most biodiverse regions of the planet.

Acknowledgements – We thank T. S. Jenkinson, and M. F. K. Becker for feedback on the manuscript; N. Pupin, A. Mesquita, E. Garcia, D. B. Delgado T. Carvalho, P. Mourao, A. F. R. Missassi, and L. F. Moreno for help with swabbing the specimens. Christopher J. Raxworthy, David Kizirian, Manoela Woitovicz Cardoso, Hélio da Silva, Moises Barbosa de Souza, José Pombal Jr., Sérgio Potsch, Taran Grant, and Ana Lúcia C. Prudente allowed access to museum specimens. Michael Forstner provided instrumentation support. Our work was funded by grants and fellowships from Conselho Nacional de Desenvolvimento Científico e Tecnológico – CNPq (#312895/2014-3 to CGB; #405285/2013-2 and #302589/2013-9 to LFT; #2013/50741-7 to CFBH) and São Paulo Research Foundation – FAPESP (#302518/2013-4 to CFBH).

References

Araujo, M. B. and Guisan, A. 2006. Five (or so) challenges for species distribution modeling. – J. Biogeogr. 33: 1677–1688.

Beaumont, L. J. et al. 2005. Predicting species distributions: use of climatic parameters in BIOCLIM and its impact on predictions of species' current and future distributions. – Biol. Model. 186: 250– 269.

Becker, C. G. and Zamudio, K. R. 2011. Tropical amphibian populations experience higher disease risk in natural habitats. – Proc. Natl Acad. Sci. USA 108: 9893–9898.

Becker, C. G. et al. 2012. Disease risk in temperate amphibian populations is higher at closed-canopy sites. – PLoS One 7: e48205.

Becker, C. G. et al. 2015. Data from: Historical dynamics of *Batrachochytrium dendrobatidis* in Amazonia. – Dryad Digital Repository, <http://dx.doi.org/10.5061/dryad.h3112>.

Berger, L. et al. 1998. Chytridiomycosis causes amphibian mortality associated with population declines in the rain forests of Australia and Central America. – Proc. Natl Acad. Sci. USA 95: 9031–9036.

Catenazzi, A. et al. 2011. *Batrachochytrium dendrobatidis* and the collapse of anuran diversity and abundance in the upper Manu National Park, southeastern Peru. – Conserv. Biol. 25: 382–391.

Cheng, T. L. et al. 2011. Coincident mass extirpation of neotropical amphibians with the emergence of the infectious fungal pathogen *Batrachochytrium dendrobatidis*. – Proc. Natl Acad. Sci. USA 108: 9502–9507.

Courtois, E. A. et al. 2015. Widespread occurrence of *Bd* in French Guiana, South America. – PLoS One 10: e0125128.

de Sá, R. O. et al. 2014. Systematics of the Neotropical genus *Leptodactylus* Fitzinger, 1826 (Anura: Leptodactylidae): phylogeny, the relevance of non-molecular evidence, and species accounts. – S. Am. J. Herpetol. 9: S1–S100.

Deichmann, J. L. et al. 2010. A note on amphibian decline in a central Amazonian lowland forest. – Biodivers. Conserv. 19: 3619–3627.

Elith, J. et al. 2006. Novel methods improve prediction of species' distributions from occurrence data. – Ecography 29: 129–151.

Elith, J. et al. 2011. A statistical explanation of MaxEnt for ecologists. – Divers. Distrib. 17: 43–57.

ESRI 2012. Arcview 10.1. – Redlands, CA.

Fisher, M. C. et al. 2009. Global emergence of *Batrachochytrium dendrobatidis* and amphibian chytridiomycosis in space, time, and host. – Annu. Rev. Microbiol. 63: 291–310.

Hijmans, R. J. et al. 2005. Very high resolution interpolated climate surfaces for global land areas. – Int. J. Climatol. 25: 1965–1978.

Hyatt, A. D. et al. 2007. Diagnostic assays and sampling protocols for the detection of *Batrachochytrium dendrobatidis*. – Dis. Aquat. Org. 73: 175–192.

IBGE 2015. Mapeamento dos recursos naturais. – <www.ibge.gov.br/home/geociencias/default_prod.shtm#REC_NAT>.

IUCN et al. 2015. Global amphibian assessment. – <www.iucnredlist.org/amphibians>.

James, T. Y. et al. 2015. Disentangling host, pathogen, and environmental determinants of a recently emerged wildlife disease: lessons from the first 15 years of amphibian chytridiomycosis research. – Ecol. Evol. 5: 4079–4097.
Kriger, K. M. et al. 2007. On the biological relevance of a single *Batrachochytrium dendrobatidis* zoospore: a reply to Smith. – Dis. Aquat. Organ. 73: 257–260.
Kulldorff, M. 1997. A spatial scan statistic. – Commun. Stat. A-Theor. 26: 1481–1496.
Kulldorff, M. 2009. Information management services. – SaTScan TM ver. 8.0: software for the spatial and space-time scan statistics, <www.satscan.org>.
Lampo, M. et al. 2006. *Batrachochytrium dendrobatidis* infection in the recently rediscovered *Atelopus mucubajiensis* (Anura, Bufonidae), a critically endangered frog from the Venezuelan Andes. – EcoHealth 3: 299–302.
Lips, K. R. et al. 2008. Riding the wave: reconciling the roles of disease and climate change in amphibian declines. – PLoS Biol. 6: e72.
Liu, X. et al. 2013. Climate, vegetation, introduced hosts and trade shape a global wildlife pandemic. – Proc. R. Soc. B 280: 20122506.
McCracken, S. et al. 2009. Detection of *Batrachochytrium dendrobatidis* in amphibians from the forest floor to the upper canopy of an Ecuadorian Amazon lowland rainforest. – Herpetol. Rev. 40: 190–195.
Menendez-Guerrero, P. A. and Graham, C. H. 2013. Evaluating multiple causes of amphibian declines of Ecuador using geographical quantitative analyses. – Ecography 36: 756–769.
Ouellet, M. et al. 2005. Historical evidence of widespread chytrid infection in North American amphibian populations. – Conserv. Biol. 19: 1431–1440.
Pounds, J. A. et al. 2006. Widespread amphibian extinctions from epidemic disease driven by global warming. – Nature 439: 161–167.
Puschendorf, R. et al. 2011. Environmental refuge from disease-driven amphibian extinction. – Conserv. Biol. 25: 956–964.
Raffel, T. R. et al. 2010. What drives chytrid infections in newt populations? Associations with substrate, temperature, and shade. – EcoHealth 7: 526–536.
Rangel, T. F. et al. 2010. SAM: a comprehensive application for spatial analysis in macroecology. – Ecography 33: 46–50.
Rödder, D. et al. 2009. Global amphibian extinction risk assessment for the panzootic chytrid fungus. – Diversity 1: 52–66.
Rodriguez, D. et al. 2014. Long-term endemism of two highly divergent lineages of the amphibian-killing fungus in the Atlantic Forest of Brazil. – Mol. Ecol. 23: 774–787.
Rohr, J. R. and Raffel, T. R. 2010. Linking global climate and temperature variability to widespread amphibian declines putatively caused by disease. – Proc. Natl Acad. Sci. USA 107: 8269–8274.
Rohr, J. R. et al. 2008. Evaluating the links between climate, disease spread, and amphibian declines. – Proc. Natl Acad. Sci. USA 105: 17436–17441.
Ron, S. R. 2005. Predicting the distribution of the amphibian pathogen *Batrachochytrium dendrobatidis* in the New World. – Biotropica 37: 209–221.
Sanderson, E. W. et al. 2002. The human footprint and the last of the wild. – Bioscience 52: 891–904.
Schloegel, L. M. et al. 2012. Novel, panzootic, and hybrid genotypes of amphibian chytridiomycosis associated with the bullfrog trade. – Mol. Ecol. 21: 5162–5177.
Soto-Azat, C. et al. 2010. Widespread historical presence of *Batrachochytrium dendrobatidis* in African pipid frogs. – Divers. Distrib. 16: 126–131.
Stevenson, L. A. et al. 2013. Variation in thermal performance of a widespread pathogen, the amphibian chytrid fungus *Batrachochytrium dendrobatidis*. – PLoS One 8: e73830.
Talley, B. L. et al. 2015. A century of *Batrachochytrium dendrobatidis* in Illinois amphibians (1888–1989). – Biol. Conserv. 182: 254–261.
USGS and FAO 2000. Global forest resources assessment (FRA 2000), global forest canopy density image. – <http://edc2.usgs.gov/glcc/fao/forest_canopy_image.php>.
Valencia-Aguilar, A. et al. 2015. The chytrid fungus acts as a generalist pathogen that infects species-rich amphibian families in Brazilian rainforests. – Dis. Aquat. Organ. 114: 61–67.
Vieira, C. A. et al. 2012. First record of *Batrachochytrium dendrobatidis* in Paraná. – Brazil. Herpet. Rev. 43: 93.
Voyles, J. L. et al. 2012. Temperature alters reproductive life history patterns in *Batrachochytrium dendrobatidis*, a lethal pathogen associated with the global loss of amphibians. – Ecol. Evol. 2: 2241–2249.
Vredenburg, V. T. et al. 2013. Prevalence of *Batrachochytrium dendrobatidis* in *Xenopus* collected in Africa (1871–2000) and in California (2001–2010). – PLoS One 8: e63791.
Weldon, C. et al. 2004. Origin of the amphibian chytrid fungus. – Emerg. Infect. Dis. 10: 2100–2105.

Supplementary material (Appendix ECOG-02055 at <www.ecography.org/appendix/ecog-02055>). Appendix 1.